PROCEEDINGS OF ECOS 2023 - THE 36TH INTERNATIONAL CONFERENCE ON
EFFICIENCY, COST, OPTIMIZATION, SIMULATION AND ENVIRONMENTAL IMPACT OF ENERGY SYSTEMS
25-30 JUNE, 2023, LAS PALMAS DE GRAN CANARIA, SPAIN

Metamodels for economically optimized closed Brayton cycles

Andreas Siman Menzel[a], Francesco Witte[b], Julio Augusto Mendes da Silva[c], Icaro Vilasboas Figueiredo[d] and Armando Sá Ribeiro Jr.[e]

[a] UFBA (Polytechnic School of UFBA), Salvador, Brazil, menzel.andreas@outlook.com, CA
[b] German Aerospace Center (DLR), Institute of Networked Energy Systems, Oldenburg, Germany, francesco.witte@dlr.de,
[c] UFBA PEI (Industrial Engineering Post-graduate Program), Salvador, Brazil, jamsilva08@gmail.com
[d] UFBA (Polytechnic School of UFBA), Salvador, Brazil, icarofvilasboas@gmail.com
[e] UFBA (Polytechnic School of UFBA), Salvador, Brazil, asrj@ufba.br

Abstract:

Closed Brayton Cycles (CBC) can be integrated with many different energy sources, such as heliothermic, biomass, geothermal, etc. However, simplified models for the cycle components are required to optimize the system in its entirety due to all possible cycle configurations like the use of recuperation, intercooling, reheating, etc, together with operating variables such as rate of heat input and its temperature. This work discusses, therefore, the development of a surrogate model for a supercritical CO_2 CBC with recuperation, intercooling and reheating. It can indicate the optimal CBC from an economic point of view under varying boundary conditions. The cycle is first optimized for different heat inputs through its operational parameters (mass flow, minimum cycle pressure and cycle pressure ratios) and heat exchangers area. Compressor and expanders costs are obtained as a function of power while heat exchangers cost is obtained as a function of their area and pressure. Each solution is used to train a surrogate model that will act as an approximator for the optimized CBC and predict cost based on heat input.

Keywords:

CBC; Economic analysis; Machine learning; Surrogate; Thermodynamic analysis.

1. Introduction

Population growth, technological and industrial development are linked to increasing demand for energy, especially in recent years. The continuous reliance on fossil fuels to meet this demand on a global scale is causing negative impacts on the environment, meaning a more robust and sustainable energy matrix is necessary. Because of this, many renewable energy sources are being searched and some of them have become economically feasible such as wind and photovoltaic thanks to continuous investment in recent years. The heliothermic energy, or Concentrating Solar Power (CSP), is one of the first solar technologies to demonstrate grid potential and that could effectively reduce carbon dioxide emissions [1, 2]. That being said, the Closed Brayton Cycle (CBC) has been gaining much attention for its efficiency and possible application as a CSP Power block [3–5].

A CBC is typically more efficient and has a lower cost per power than more conventional cycles such as Rankine and Organic Rankine for heat sources in a temperature range of 600 to 1000°C [6–8]. The CBC also favours the construction of plants in arid locations with higher levels of insolation, i.e., no water is needed, thus being ideal for power generation with CSP.

Variations of the closed Brayton cycle using CO_2 as working fluid at supercritical condition (S-CO_2) are usually studied for heliothermic sources. They are dominant in the few works available in the literature on the use of CBCs to harness solar thermal energy below 600C [8–12]. This is because the closed Brayton cycle with minimum temperature and pressure values near the critical point of the working fluid experience a large reduction in compression work, increasing the thermal efficiency of the cycle [13]. The use of CO_2 as a working fluid stems from the proximity of its critical temperature ($T_c = 31.1$°C) to the ambient temperature [9–11].

The compatibility of CBC with heat sources below 600°C is uncertain. Garg et al [14] investigate a supercritical Brayton cycle using CO_2 with an efficiency potentially greater than 30% even for 820 K (~547°C)

https://doi.org/10.52202/069564-0119

sources. Milani et al. [11] evaluated several configurations of a Brayton Cycle using supercritical CO_2 as the working fluid for a hybridized CSP power source. The optimal configuration has a turbine inlet temperature (TIT) of 600°C and can reach a thermal efficiency of 52.7%. Utamura and Tamaura [9] studied the application of a CBC with S-CO_2, recuperation and pre-and inter-cooling in solar thermal sources with a TIT of up to 577°C. The authors found that the cycle can reach thermal efficiencies of up to 47%.

A widely explored option to optimize the performance of the closed Brayton cycle is the use of multistage (intercooling and/or reheating) compression and expansion plus recuperation. This is a common way to increase efficiency and reduce irreversibilities, which can improve the applicability of the cycle at heat source temperatures below 600C [15, 16]. In this case, a small pressure ratio enables high thermal efficiency and increases the recuperation potential, decreasing the size of the recuperator that would be required for a single-stage cycle.

The use of multistage compression and expansion will require the evaluation of multiple configurations of the cycle to determine the optimal or most economically feasible one. The optimization uses input data from the available heat source, i.e., inlet temperature and mass flow rate of the heat source fluid, as well as the rate in which heat is supplied. However, evaluating all possible configurations for each instance of the decision variables, like heat exchanger area, turbine inlet temperature, pressure ratio, etc., in the optimization process is computationally expensive. Thus, this work proposes an alternate method of optimization using Surrogates to reduce the processing time of the optimal CBC configuration while maintaining convergence to a global minimum specific cost value. Surrogate models, also known as metamodels, response surfaces, approximation models, etc., map an input-output relationship from data associated with some phenomenon to reproduce it in an approximate and often faster way [17, 18].

Using metamodels for complex process optimization is common for several engineering disciplines. Urquhart et al. [19] investigate the performance of two methods based on the construction of response surfaces for the optimization of aerodynamic shapes. Huang et al. [20] propose and study the use of Kriging models to perform global optimizations of stochastic systems. Carranza-Abaid et al. [21] created thermodynamically consistent Machine Learning-based Surrogate models to represent phase equilibria with multiple components.

In this work, a surrogate is created to replace the overall CBC model, reducing computational time, and allowing its use in broader optimization codes.

2. System Description

2.1. CBC Layout

Figure 1 displays a schematic of the proposed S-CO_2 CBC, while Fig. 2. shows its T-s diagram. The thermal and working fluids used are DOWTHERM A (in red) and CO_2 (in black), respectively. The optimal configuration and operating condition of the CBC varies depending on: (i) thermal fluid inlet temperature (T_Q^{in}); (ii) thermal fluid mass flow rate ($\dot{m}_Q$); and (iii) total heat transfer rate ($\dot{Q}_H = \dot{Q}_{H,0} + \dot{Q}_{H,1}$).

The working fluid at supercritical pressures goes through the compression process with intercooling (1-4) and then to the recuperator (4-5) as a cold stream. In the recuperator its temperature is increased by residual heat from the working fluid after expansion process. The CO_2 is heated up to turbine inlet temperature - TIT (5-6) before entering the re-heated expansion system (6-9) and the recuperator as hot stream (9-10). The working fluid is then cooled in (10-1) and returns to the cycle starting point (1).

The thermal fluid enters the reheaters and the main heat exchanger with the same temperature (T_Q^{in}). Different mass flow rates and output temperatures are allowed, which serve as decision variables chosen during optimization. The lower and upper boundaries of each global input are shown on Table 1.

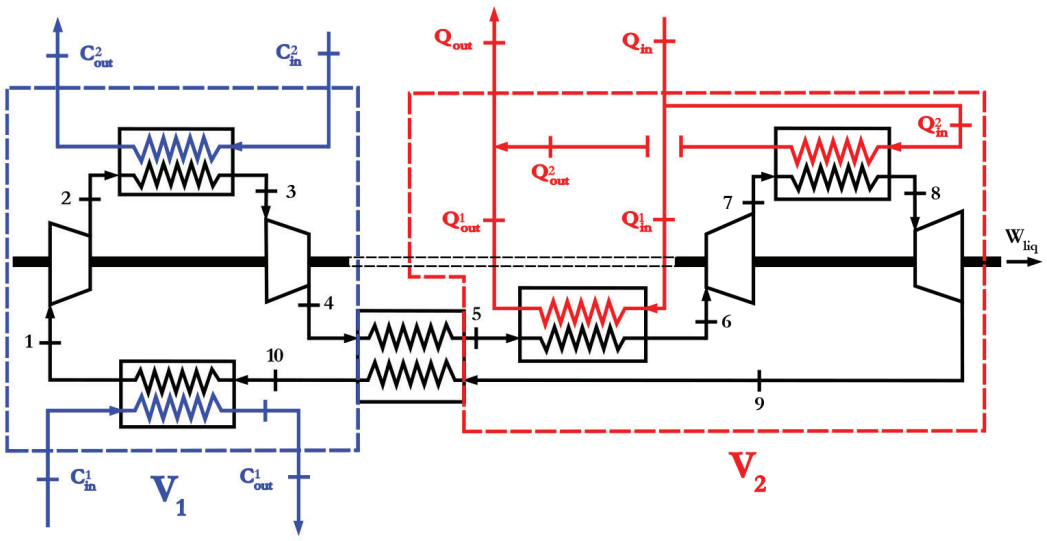

Figure 1. CBC diagram with supercritical CO_2.

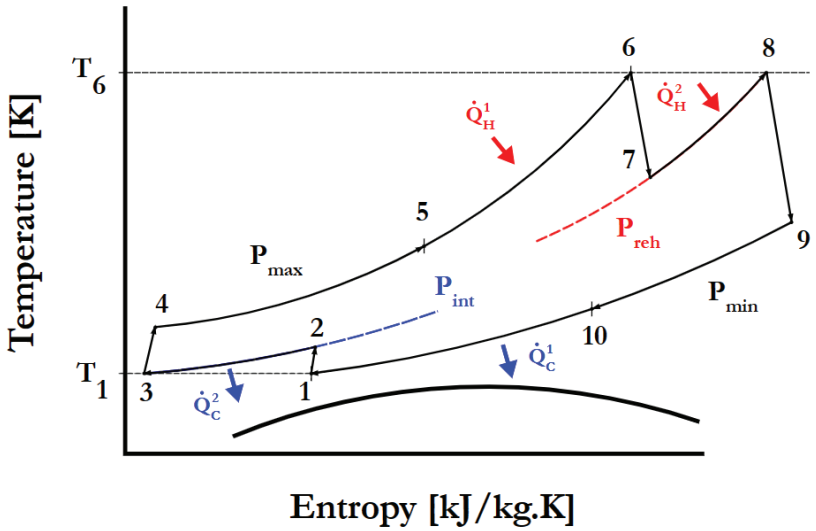

Figure 2. T-s diagram of CBC with supercritical CO_2.

Table 1. Operating range of the CBC input parameters.

	Lower boundary	Upper boundary
T_Q^{in}	200°C	390°C
$\dot{m}_Q$	100 kg/s	200 kg/s
$\dot{Q}_H$	100 kW	50000 kW

https://doi.org/10.52202/069564-0119

3. Thermodynamic Modelling

All components were modelled in a permanent regime, disregarding kinetic and potential energy effects and pressure drop in heat exchangers and piping. Table 2 presents the fixed parameters considered in the calculation of the thermodynamic states for CBC [22–24].

Table 2. Fixed parameters used to model CBC.

	Description	Value
$\eta_{ise,comp}$	Isentropic Compressor Efficiency	85%
$\eta_{ise,turb}$	Isentropic Turbine Efficiency	85%
η_e	Generator Efficiency	95%
T_C^{in}	Cooling Water inlet temperature	35°C
T_C^{out}	Cooling Water outlet temperature	42.55°C
$\overline{U}_{g/g}$	Overall heat transfer coefficient (gas/gas)	47.5 $W/(m^2 \cdot K)$
$\overline{U}_{g/w}$	Overall heat transfer coefficient (gas/water)	177.5 $W/(m^2 \cdot K)$
$\overline{U}_{g/o}$	Overall heat transfer coefficient (gas/oil)	274.5 $W/(m^2 \cdot K)$

The isentropic efficiencies of the compressor ($\eta_{ise,comp}$) and turbine ($\eta_{ise,turb}$) are calculated according to Eqs. (1) - (2), respectively. Their energy balances are represented by Eqs. (3) - (4). The energy balance of the recuperator is presented by Eq. (5) and assumes no heat losses to the environment.

$$\eta_{ise,comp} = \frac{h_{2s} - h_1}{h_2 - h_1} = \frac{h_{4s} - h_3}{h_4 - h_3} \quad (1)$$

$$\eta_{ise,turb} = \frac{h_6 - h_7}{h_6 - h_{7s}} = \frac{h_8 - h_9}{h_8 - h_{9s}} \quad (2)$$

$$\dot{W}_{turb,n} = \dot{m}_{CO2}(h_{in} - h_{out}) \quad (3)$$

$$\dot{W}_{comp,n} = \dot{m}_{CO2}(h_{out} - h_{in}) \quad (4)$$

$$\dot{m}_{CO2}(h_5 - h_4) = \dot{m}_{CO2}(h_9 - h_{10}) \quad (5)$$

Equations (6) - (7) show the energy balances of the cycle remaining heat exchangers.

$$\dot{m}_{CO2}(h_{out} - h_{in}) = \dot{m}_Q\left(h_{in}^Q - h_{out}^Q\right) \quad (6)$$

$$\dot{m}_{CO2}(h_{in} - h_{out}) = \dot{m}_{water}(h_{water}^{out} - h_{water}^{in}) \quad (7)$$

Liquid electric power ($\dot{W}_{liq}$) and cycle total efficiency (η_t) are given by Eqs. (8) – (10).

$$\dot{W}_{liq} = \sum_{i=1}^{n} \dot{W}_{turb,i} - \sum_{i=1}^{n} \dot{W}_{comp,i} \quad (8)$$

$$\dot{W}_{liq,e} = \eta_e \dot{W}_{liq} \quad (9)$$

$$\eta_e = \frac{\dot{W}_{liq,e}}{\dot{Q}_H} \quad (10)$$

Equations (11) – (13) are used to calculate the area for each heat exchanger present in the cycle.

$$\begin{cases} \Delta T_{in} = T_h^{in} - T_c^{out} \\ \Delta T_{out} = T_h^{out} - T_c^{in} \end{cases} \quad (11)$$

$$\Delta T_{ml} = (\Delta T_{out} - \Delta T_{in})/ln(\Delta T_{out}/\Delta T_{in}) \quad (12)$$

$$A_{hx} = \frac{\dot{Q}_H}{\overline{U} \cdot \Delta T_{ml}} \quad (13)$$

Most of the working fluid's thermodynamic properties were calculated through the use of CoolProp, a module dedicated to the calculation of thermodynamic states, and TesPy, a thermodynamic cycle simulation toolkit that was used to model the different components of the proposed CBC configuration [25, 26].

4. Economic Models

According to the literature, there are many different methods to estimate the acquisition cost of industrial equipment [27, 28]. The cost estimates in this work came from Eq. (14) of exponential cost of Bejan et al. [27]. Cost data from Peters et al. [28] for a centrifugal compressor, axial turbine and double-pipe and U-tube heat exchangers was used to adjust the equation.

$$C = C_{ref}\left(\frac{X}{X_{ref}}\right)^{\alpha}\left(\frac{CEPCI}{CEPCI_{ref}}\right) \quad (14)$$

Equation (14) indicates the equipment acquisition cost (C) using reference values for equipment size (X_{ref}) and cost (C_{ref}), the current size parameter (X) and an adjustable exponent (α). The ratio between $CEPCI$ (Chemical Engineering Plant Cost Index) and $CEPCI_{ref}$ serves as a correction factor for the cost of equipment in years other than the base year, which in this case is the year 2021 with $CEPCI_{ref} = 607.5$.
The total acquisition cost of CBC encompassing compression and expansion systems, is obtained by summing their respective individual equipment costs.
Table 3 displays the cost parameters of compressors and turbines used in the CBC. The heat exchangers acquisition cost varies according to the thermal load, operating pressure, and area. Tables 4 - 5 present the operational ranges in which each heat exchanger type has the lowest cost per area [27, 28].

Table 3. Cost estimation parameters for compression and expansion equipment.

Equipment	Size Parameter	Reference Size	Reference Cost [$]	α
Axial Turbine	Electric Power	10 kWe	16955.23	0.611
Centrifugue Compressor	Electric Power	100 kWe	105240.35	0.943

Table 4. General cost estimation parameters for heat exchangers.

Type	Exchanger Area [m²]	Size Parameter	Reference Size [m²]	α
Double-Pipe	0.25 – 20	Exchanger Area [m²]	0.25	0.063
U-Tube	20 – 1000	Exchanger Area [m²]	20	0.479

https://doi.org/10.52202/069564-0119

Table 5. Operating conditions and reference cost for heat exchangers.

Type	Pressure Range [MPa]	Reference Cost [$]
Double-Pipe	10 – 20	2321.89
	20 – 30	3605.73
	30 – 40	5494.36
U-Tube	10 - 20	9831.35
	20 – 30	10591.46
	30 - 40	11015.60

The cheapest heat exchangers were investigated and selected based on cost data from Peters et al. [28]. Figure 3 compares the specific cost curves of the cheapest exchangers with an operational pressure from 0.1 to 5 MPa. The plate exchangers (Welded and Gasketed Plate) have the lowest specific cost. However, their operating pressure limit goes up to 2.5 MPa, thus, in operating pressures above this value, Double-Pipe and U-Tube exchangers may be required.

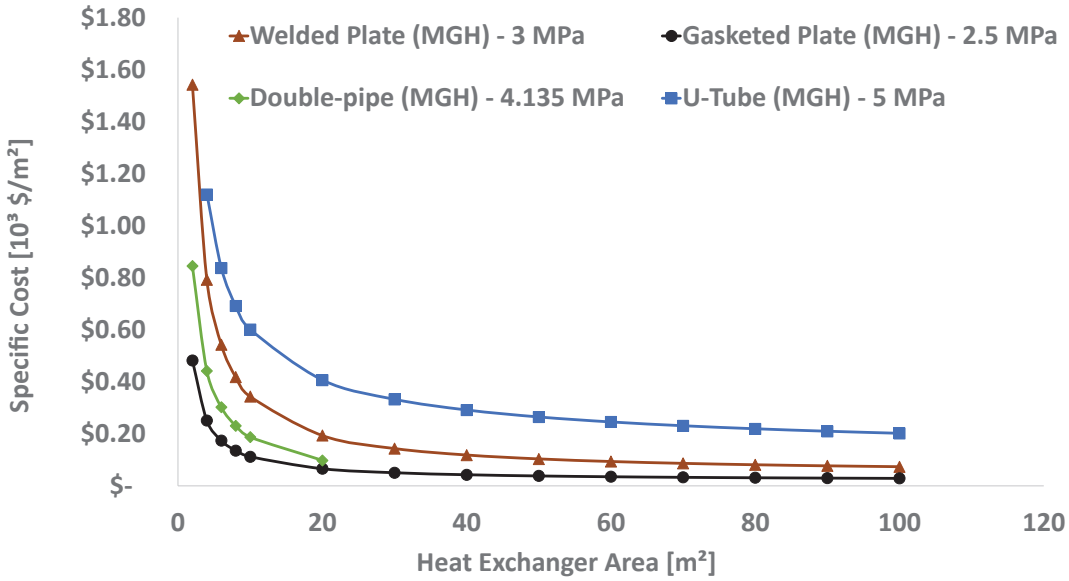

Figure 3. Specific cost curves comparison of different types of heat exchangers with operating pressure between 0.1 – 5 MPa.

5. CBC Optimization

The optimal cycle considered in this work is the one that has the greatest energy output for the lowest acquisition cost for its given heat input. Therefore, the CBCs objective function to be minimized is its specific cost, as per Eq. (15).

$$\min C_{e,CBC} = \frac{C_{total}}{\dot{W}_{liq,e}} \tag{15}$$

The optimizations were performed using Particle Swarm Optimization, implemented through the Pygmo library in Python, developing 50 individuals over a course of 30 generations [29, 30]. To facilitate data transfer between the power plant simulation in TESPy and the optimization a dedicated API was developed based on the work of Chen et al. [31] and made available in the most recent version of the software [32].

https://doi.org/10.52202/069564-0119

Many decision variables with general boundaries have been initially considered in the optimization process, such as working fluid mass flow rate, minimum cycle pressure, compression and expansion pressure ratios, thermal fluid split value between the heater and reheater, minimum temperature difference in the recuperator, main heater, and cooler, etc. To restrict their boundaries, 25 runs resulting in 25 champions have been performed and each of the decision variables was plotted against the obtained objective function values. The variables whose variation was of no consequence to the final result were set to a specific value. The final set of decision variables can be found in Table 6.

Table 6. Decision variables considered.

Decision Variable	Description	Value Interval
P_{min}	Minimum cycle pressure	10.1 – 13.0 MPa
ΔP	Total cycle pressure variation	2.0 – 8.0 MPa
$\dot{m}_{CO2}$	CO_2 mass flow rate	100.0 – 350.0 kg/s
ΔT_{min}^{reh}	Minimum Reheater temperature difference	3.0-20.0 ºC
f_q	Thermal fluid mass flow rate fractions	0 - 1
P_{int}^{comp}	Compression system intermediate pressures	P_{min} - P_{max} MPa
P_{int}^{exp}	Expansion system intermediate pressures	P_{min} - P_{max} MPa

6. Surrogate Model Development

This work used Scikit-Learn, one of the most used Machine Learning (ML) libraries in Python [33], to build the CBCs response surface. This approach used a supervised learning model with offline training. Unsupervised learning was implemented for dimensionality reduction of each model training set [34–36]. A regression model was trained on the champion population obtained as a result of the optimization process to predict the value of optimum specific cost for a given set of input variables.

Dimensionality reduction was performed using a Stratified Latin Hypercube (LHS) with *CenterMaximin* from the PyDOE2 library in Python which is a widely used technique in surrogate modelling [17, 37–39]. LHS is, by itself, used to generate smaller data sets with more information. *CenterMaximin* is a stratification criterion that allows LHS to further spread out those samples within their data regions [18, 37].

The surrogate was built using linear regression with a polynomial and a normalizing pre-processing step. These steps highlights trends and relationships in the data previously unknown to the ML model, augmenting their capacity [36, 40, 41]. The model was validated using *Cross-Validation* [17, 18, 36] which allows the exploration of the entire data set for both training and validation, through the use of an R^2 score.

7. Results and Discussion

7.1. Optimization Results

A total of 832 champions were obtained through the optimization process with an average of 8 champions/hour while using an Intel Core i7 processor computer with 16 GB of RAM memory and 8 logic cores. Although the champions are not always guaranteed to be global optima, they can still be used to verify the thermodynamic consistency of the developed objective function. As shown in Figure 4, the obtained values of specific cost tend to decrease with greater values of thermal input to the cycle, when considering a constant average heat source temperature of $200°C$. Figure 5 highlights that the optimum cycle efficiency tends to increase with a higher average heat source temperature, considering a constant Heat input of $20000\ kW$, as was to be expected.

https://doi.org/10.52202/069564-0119

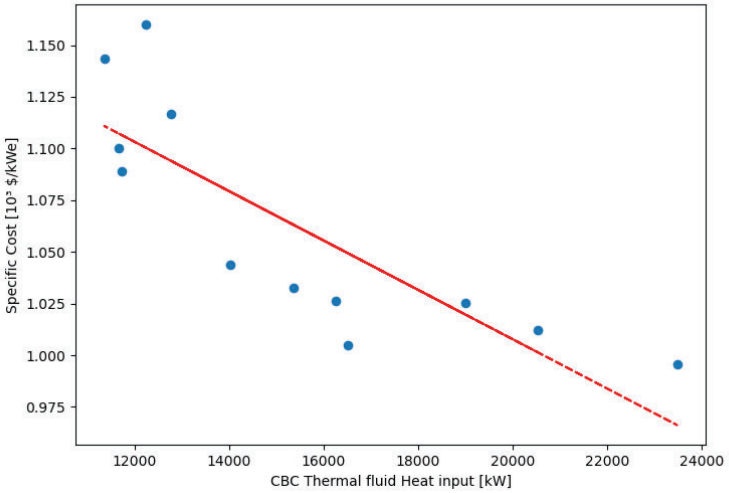

Figure 4. Specific cost versus CBC heat input, considering an average heat source temperature at 200°C.

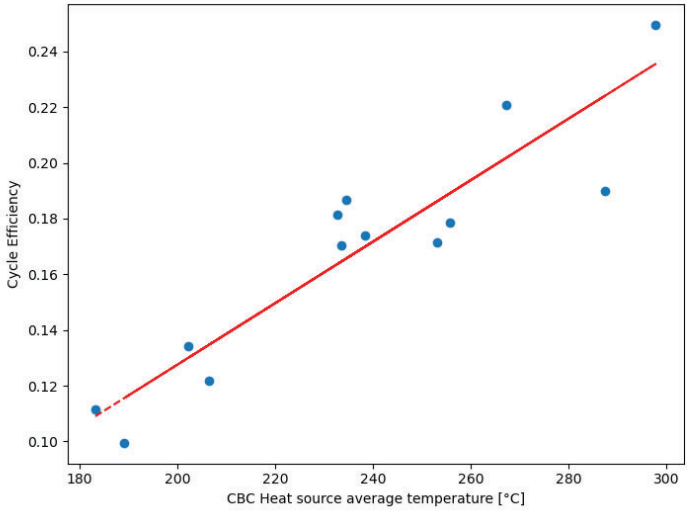

Figure 5. Optimum cycle efficiency versus heat source average temperature, considering a heat input of 20000 kW.

7.2. Surrogate Results

The most informative input format for training the Surrogate model was shown to be a combination of the original input variables (T_Q^{in}, $\dot{m}_Q$ and $\dot{Q}_H$) and implicit variables, calculated considering that the heat fluid possesses a constant pressure of $P_Q = 10.49\ MPa$, such as outlet thermal fluid temperature (T_Q^{out}) and the arithmetic average of the heat source temperature ($\overline{T}_Q$). Figure 6 is a correlation plot of each set of values for the mentioned variables and their respective optimal specific cost.

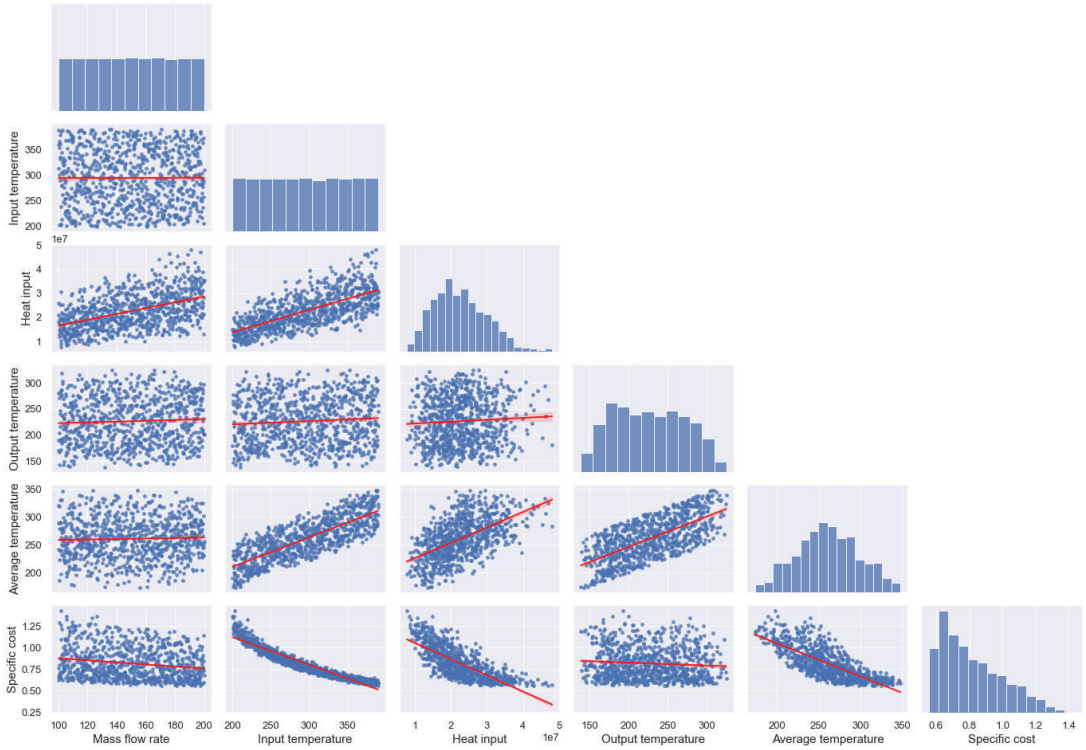

Figure 6. Correlation and distribution plot between Thermal fluid input variables (mass flow rate, input temperature, heat input, output temperature and average temperature) and optimum CBC specific cost.

Using variables with a clear relationship to the objective tend to improve the final cross-validation score of the model [34, 36].

The regression Model in question is of the second degree and utilizes a normalizing pre-processing feature from Scikit-Learn to allow for a model with a higher R^2. All champions have been used to train the model, with its final cross-validation score being $R^2 = 0.9911 \pm 0.0022$. Figures 7(a) and (b) display the residuals and prediction versus real value plots for the trained model when predicting its training set, respectively. While the model has a precision score of 99.11%, there is still an amount of residual error that varies in its majority between $(-150, 50)$ $\$/kW_e$. The model took approximately 0.004 s to predict the specific cost of 832 different sets of input variables.

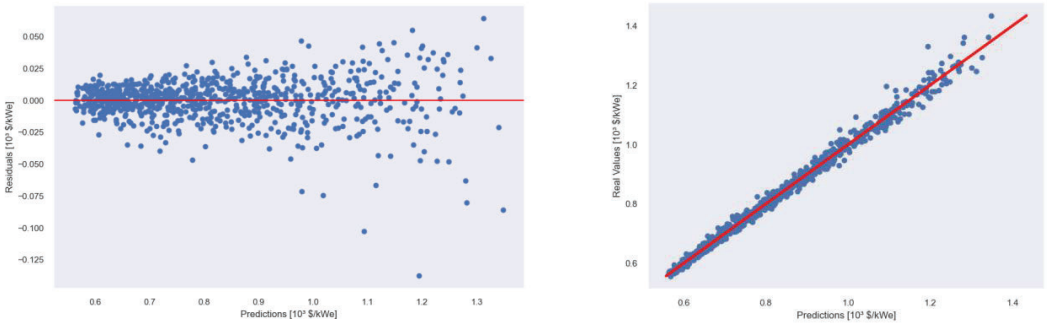

(a) *(b)*

Figure 7. Surrogate model (a) specific cost prediction residual plot, (b) specific cost prediction versus real values plot.

https://doi.org/10.52202/069564-0119

The created surrogate model is shown to be much faster to determine the optimum minimal specific cost of the CBC than the optimization method, at a very low precision cost, even though it only utilized 832 Champions to be created. The method presented in this work allowed for the creation of a deployable representation of the proposed Thermodynamic cycle that, while in this case was used to investigate the minimal specific cost, could also be used to evaluate other parameters of interest, such as number of intercoolers/reheaters, maximum cycle pressure, etc. as a function of a set of input variables.
It should be noted that an interesting application would be to use the model to perform a preliminary evaluation of the solution space for optimum CBC configuration and then perform a single optimization on the region most inclined to contain the minimum. This way the global solution space can be more thoroughly investigated at a very low computational burden. It should also be brought to attention that optimum CBC configurations can have a typical specific cost ranging from 600 to $1400\ \$/kW_e$ under the proposed ranges of input variables. Therefore, the closed Brayton cycle with Heat input from a low temperature source might be economically feasible given the right conditions.

8. Conclusion

The present work has shown that it is possible to create estimators that can allow for precise evaluations of a supercritical CBC using intercooling, reheating and a recuperator. First, the proposed cycle was optimized for multiple combinations of input variables, i.e. thermal fluid input temperature, mass flow rate and exchanged heat, so as to minimize the cycle's specific cost. After 832 champions were acquired, they were used to train a surrogate model that predicts optimum specific cost for the CBC based on a set of input variables. The difference in time between the optimization and the evaluation through the surrogate model on the specified machine is in the order of $10^8 s$. With a 99.11% cross-validation score, it can be considered as a viable estimator for the supercritical CBC.

Acknowledgements

The authors would like to thank Grupo Global Participações em Energia (GPE) for the financial support under Agência Nacional de Energia Elétrica (ANEEL) P&D program, project number PD-06961-0011/2019.

References

[1] Goswami DY. *Principles of solar engineering*. 3rd ed. Boca Raton: CRC Press, 2015.

[2] Santos JJCS, Palacio JCE, Reyes AMM, et al. Concentrating Solar Power. In: *Advances in Renewable Energies and Power Technologies*. Elsevier, pp. 373–402.

[3] Iverson BD, Conboy TM, Pasch JJ, et al. Supercritical CO2 Brayton cycles for solar-thermal energy. *Appl Energy* 2013; 111: 957–970.

[4] Khatoon S, Kim MH. Potential improvement and comparative assessment of supercritical Brayton cycles for arid climate. *Energy Convers Manag* 2019; 200: 112082.

[5] Mahmoudi SMS, Akbari AD, Rosen MA. Thermoeconomic analysis and optimization of a new combined supercritical carbon dioxide recompression Brayton/Kalina cycle. *Sustain*; 8. Epub ahead of print 2016. DOI: 10.3390/su8101079.

[6] Najjar YSH, Zaamout MS. Comparative performance of closed cycle gas turbine engine with heat recovery using different gases. *Heat Recover Syst CHP* 1992; 12: 489–495.

[7] Yu SC, Chen L, Zhao Y, et al. A brief review study of various thermodynamic cycles for high temperature power generation systems. *Energy Convers Manag* 2015; 94: 68–83.

[8] Dunham MT, Iverson BD. High-efficiency thermodynamic power cycles for concentrated solar power systems. *Renew Sustain Energy Rev* 2014; 30: 758–770.

[9] Utamura M, Tamaura Y. A solar gas turbine cycle with super-critical carbon dioxide as a working fluid. *Proc ASME Turbo Expo* 2006; 4: 329–335.

[10] Rovira A, Muñoz-Antón J, Montes MJ, et al. Optimization of Brayton cycles for low-to-moderate grade thermal energy sources. *Energy* 2013; 55: 403–416.

[11] Milani D, Tri M, Mcnaughton R, et al. Optimizing an advanced hybrid of solar-assisted supercritical CO 2 Brayton cycle : A vital transition for low-carbon power generation industry. *Energy Convers Manag* 2017; 148: 1317–1331.

[12] Binotti M, Astolfi M, Campanari S, et al. Preliminary assessment of sCO2 cycles for power generation in CSP solar tower plants. *Appl Energy* 2017; 204: 1007–1017.

[13] Invernizzi CM. Prospects of mixtures as working fluids in real-gas Brayton cycles. *Energies*; 10. Epub

ahead of print 2017. DOI: 10.3390/en10101649.

[14] Garg P, Kumar P, Srinivasan K. The Journal of Supercritical Fluids Supercritical carbon dioxide Brayton cycle for concentrated solar power. *J Supercrit Fluids* 2013; 76: 54–60.

[15] Le Roux WG, Bello-Ochende T, Meyer JP. A review on the thermodynamic optimisation and modelling of the solar thermal Brayton cycle. *Renew Sustain Energy Rev* 2013; 28: 677–690.

[16] Mohammadi K, McGowan JG, Saghafifar M. Thermoeconomic analysis of multi-stage recuperative Brayton power cycles: Part I- hybridization with a solar power tower system. *Energy Convers Manag* 2019; 185: 898–919.

[17] Jiang P, Zhou Q, Shao X. *Surrogate-Model-Based Design and Optimization*. 2020. Epub ahead of print 2020. DOI: 10.1007/978-981-15-0731-1_7.

[18] Forrester AIJ, Sóbester A, Keane AJ. *Engineering Design via Surrogate Modelling*. 2008. Epub ahead of print 2008. DOI: 10.1002/9780470770801.

[19] Urquhart M, Ljungskog E, Sebben S. Surrogate-based optimisation using adaptively scaled radial basis functions. *Appl Soft Comput J* 2020; 88: 106050.

[20] Huang D, Allen TT, Notz WI, et al. Global optimization of stochastic black-box systems via sequential kriging meta-models. *J Glob Optim* 2006; 34: 441–466.

[21] Carranza-Abaid A, Svendsen HF, Jakobsen JP. Surrogate modelling of VLE: Integrating machine learning with thermodynamic constraints. *Chem Eng Sci X* 2020; 8: 100080.

[22] Çengel YA, Ghajar AJ. *Heat and Mass Transfer*.

[23] Kakaç S, Liu H, Pramuanjaroenkij A. *Heat Exchangers: Selection, Rating, and Thermal Design, Third Edition*. 2012.

[24] Shah RK, Sekuli DP. *Selection of Heat Exchangers and Their Components*. 2007. Epub ahead of print 2007. DOI: 10.1002/9780470172605.ch10.

[25] Witte F, Tuschy I. TESPy: Thermal Engineering Systems in Python. *J Open Source Softw* 2020; 5: 2178.

[26] Bell IH, Wronski J, Quoilin S, et al. Pure and Pseudo-pure Fluid Thermophysical Property Evaluation and the Open-Source Thermophysical Property Library CoolProp. Epub ahead of print 2014. DOI: 10.1021/ie4033999.

[27] Bejan A, Tsatsaronis G, Moran M. *Thermal Design and Optimization*. 1st ed. John Wiley & Sons, Inc., 1995.

[28] Peters MS, Timmerhaus KD, West RE. *Plant Design and Economics for Chemical Engineers*. 5th ed. 2003. Epub ahead of print 2003. DOI: 10.16309/j.cnki.issn.1007-1776.2003.03.004.

[29] Arora JS. *Introduction to Optimum Design*. 4th ed. Elsevier. Epub ahead of print 2017. DOI: 10.1016/C2013-0-15344-5.

[30] Biscani F, Izzo D. A parallel global multiobjective framework for optimization: pagmo. *J Open Source Softw* 2020; 5: 2338.

[31] Chen C, Witte F, Tuschy I, et al. Parametric optimization and comparative study of an organic Rankine cycle power plant for two-phase geothermal sources. *Energy* 2022; 252: 123910.

[32] Witte F. TESPy: Thermal Engineering Systems in Python. Epub ahead of print 2022. DOI: 10.5281/ZENODO.7134696.

[33] Pedregosa F, Varoquaux G, Gramfort A, et al. Scikit-learn: Machine Learning in Python. *J Mach Learn Res* 2011; 2825–2830.

[34] Goodfellow I, Bengio Y, Courville A. *Deep Learning*. 2017.

[35] Bishop CM. *Pattern Recognition and Machine Learning*. Springer, 2006. Epub ahead of print 2006. DOI: 10.13109/9783666604409.185.

[36] Hastie T, Tibshirani R, Friedman J. *The Elements of Statistical Learning - Data Mining, Inference, and Prediction*. 2008. Epub ahead of print 2008. DOI: 10.1007/978-0-387-84858-7.

[37] Garud SS, Karimi IA, Kraft M. Design of computer experiments: A review. *Comput Chem Eng* 2017; 106: 71–95.

[38] Jin R, Chen W, Sudjianto A. On sequential sampling for global metamodeling in engineering design. *Proc ASME Des Eng Tech Conf* 2002; 2: 539–548.

[39] Giunta AA, Wojtkiewicz SFJ, Eldred MS. Overview of Modern Design of Experiments Methods for Computational Simulations. *41st Aerosp Sci Meet Exhib* 2003; 1–18.

[40] Koziel S, Yang X-S. *Computational Optimization, Methods and Algorithms*. Springer Berlin Heidelberg, 2011.

[41] García S, Luengo J, Herrera F. *Data Preprocessing in Data Mining*. 2015.

https://doi.org/10.52202/069564-0119